Journal of Electrochemical Science and Technology
Vol. 1, No. 2, 2010, 85-91
DOI:10.5229/JECST.2010.1.2.085

Journal of Electrochemical Science and Technology

Reaction Behavior of $Li_{4+x}Ti_5O_{12}$ Anode Material as Depth of Discharge

Woosuk Cho, Jun Ho Song, Min-Sik Park, Jae-Hun Kim, Jeom-Soo Kim and Young-Jun Kim†
Advanced Batteries Research Center, Korea Electronics Technology Institute, #68 Yatap-dong, Bundang-gu, Seongnam-si, Gyeonggi-do 463-816, Korea

ABSTRACT :

We have studied the origin of an additional plateau of $Li_{4+x}Ti_5O_{12}$ (LTO) observed at 0.7 V (vs. Li/Li^+). Some LTO has to be discharged down to below 1.0 V forming two-stage plateau (1.5 V and 0.7 V) in order to obtain most of capacity while others could achieve the same level of capacity at higher potential (1.0 V vs. Li/Li^+) forming one plateau (1.5 V). The particle size effect has been investigated as a possible reason of this. The 0.7 V plateau was gradually elongated with increasing the particle size. The structural variations and kinetic behaviors during discharge were carefully examined by *in-situ* XRD technique and OCV measurement. According to structural and electrochemical verifications, the kinetic limitation of Li^+ insertion is responsible primarily for the two-stage plateau which is related to the particle size of LTO rather than the formation of new intermediate phase during discharge. Herein, we propose a possible reaction model to elucidate this abnormal behavior of LTO below 1.0 V (Li/Li^+).

Keywords : Li-ion batteries, Lithium titanate, Spinel, *in-situ* XRD, Biphasic reaction.

Received December 13, 2010 : Accepted December 24, 2010

1. Introduction

Lithium titanates, $Li_{4+x}Ti_5O_{12}$, have been drawn much attention as a promising anode material for lithium ion batteries because of its excellent structural stability on Li^+ insertion and extraction reaction.[1-2] The spinel $Li_4Ti_5O_{12}$ having a cubic symmetry belongs to the space group of $Fd\bar{3}m$. Li^+ are located in channel (tetrahedral 8a) and framework (octahedral 16d) structural parts, respectively. The octahedral 16d sites are occupied with Li and Ti with a molar ratio of 1 : 5 for each formula unit ($Li_4Ti_5O_{12}$) as described in Fig. 1. It is believed that the Li^+ in 16d sites are fixed and not movable in this system.[3)]

In crystallographic point of view, Li^+ are occupied in 8a sites forming a spinel structure at the initial stage of discharge ($Li_{4+x}Ti_5O_{12}$, $x = 0$). As the lithium insertion (discharge) proceeds, inserted Li^+ are located at 16c sites. Simultaneously, the Li^+ ions initially located in 8a sites are transported to 16c sites, leading to the phase transition of $Li_{4+x}Ti_5O_{12}$ from spinel to rock-salt structure.[3-5)] Both structures can be expressed as follows;

$Li_{3(8a)}[LiTi_5]_{(16d)}O_{12(32e)}$: Spinel

$Li_{6(16c)}[LiTi_5]_{(16d)}O_{12(32e)}$: Rock-salt

A plateau observed at 1.56 V (vs. Li/Li^+) is a general characteristic of $Li_{4+x}Ti_5O_{12}$ caused by the two-phase reaction between spinel and rock-salt phases according to Gibbs phase rule. 3 mol of Li^+ can be inserted into $Li_{4+x}Ti_5O_{12}$ during discharge process until the cell voltage reaches to 1.0 V. At the same time, the spinel phase is changed into the rock-salt phase via two-phase region

†Corresponding author. Tel.: +82-31-789-7490
E-mail address: yjkim@keti.re.kr

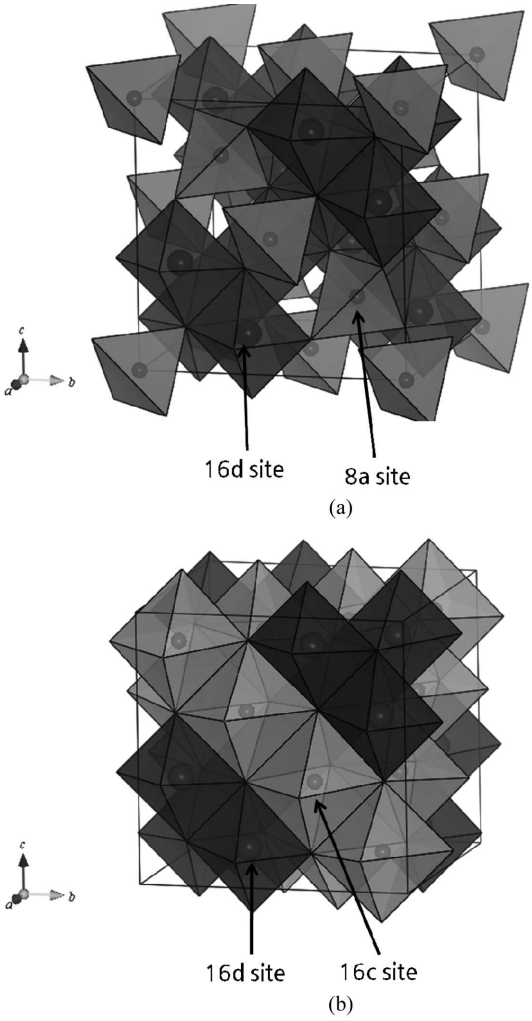

Fig. 1. Crystal structure of $Li_{4+x}Ti_5O_{12}$: (a) $Li_4Ti_5O_{12}$, spinel structure; Li ions are occupied in 8a tetrahedral sites and (b) $Li_7Ti_5O_{12}$, rock-salt structure; Li ions are occupied in 16c octahedral sites.

by electrochemical Li^+ insertion into 16c sites accompanied with a relocation of initially occupied Li^+ in 8a sites to 16c sites.[3] Beside this main plateau, another plateau was observed below 1.0 V (vs. Li/Li^+).[6-9] Those reports speculated the formation of new phase by an order/disorder transition as a possible reason. Recently, X.L. Yao *et al*. also reported an additional plateau around 0.7 V (vs. Li/Li^+) with explanation of a core/shell structure model and carbon-triggered-capacity effect.[10] However, an exact formation mechanism for the additional plateau around 0.7 V has not been fully understood yet.

In this study, authors have synthesized LTOs having various particle size to clarify the origin of low voltage plateau (0.7 V vs. Li/Li^+). Characteristics of synthesized powder were investigated with respect to the electrochemical kinetics and structural change. A reaction model is proposed to elucidate the low voltage plateau of LTO.

2. Experimental

Commercial grade nano-sized $Li_4Ti_5O_{12}$ (LTO) powder was used as a reference material. The LTO with different particle sizes were prepared by a simple thermal treatment of the nano-sized LTO powder at 700°C, 800°C and 900°C for 12 h under air atmosphere. Powder X-ray diffraction (XRD) and *in-situ* XRD patterns were obtained using a D8-Brucker diffractometer equipped with a monochromated Cu Kα radiation (λ = 1.54056 Å). The morphology of the powders was observed by field emission scanning electron microscope (FE-SEM, JEOL JSM-7000F). The *in-situ* XRD was performed using a lab-made in-situ cell. The electrode of in-situ cell was a mixture of active material powders (80 wt.%), carbon black (Super P, 10 wt.%), and poly(tetrafluoroethylene) (PTFE) binder. Li metal foil was used as a counter electrode and 1 M $LiPF_6$ in ethylene carbonate (EC)/diethyl carbonate (DEC) (1 : 1 volume ratio, Panax Etec Co. LTD) as an electrolyte. Li^+ insertion and extraction were performed by potentiostatic methods.

The electrodes were prepared by coating slurries containing active material powders (80 wt.%), carbon black (Super P, 10 wt.%), and polyvinylidene fluoride (PVDF) dissolved in *n*-metyl-2-pyrolidinone (NMP) on copper foil substrates. After coating, the electrodes were pressed and dried for 12 h at 120 °C. The CR 2032 coin-type cells were assembled in a dry room which dew point was controlled less than –45 °C. The cells consisted of the $Li_4Ti_5O_{12}$ working electrode, a Li metal foil as a counter electrode, a porous polyethylene membrane as a separator, and 1 M $LiPF_6$ in ethylene carbonate (EC)/diethyl carbonate (DEC) (1 : 1 volume ratio, Panax Etec Co. LTD) as an electrolyte. The discharge (lithiation)-charge (de-lithiation) experiments were performed galvanostatically at a constant current between C/10 and 2 C using a TOSCAT-3100U cycler (Toyo system Co.) at room temperature. Open circuit voltage was measured with a three-electrode type cell. Li metal foil was used as counter and ref-

erence electrode. Li^+ insertion was progressed with a rate of C/20 then relaxed for 6 h.

3. Results and Discussion

It has been reported that the electrochemical properties of materials are highly depending on their thermodynamic and kinetic nature.[11,12] The correlation between the particle size and the electrochemical behavior has been investigated in order to identify an electrochemical reaction mechanism of LTO below 1.0 V (vs. Li/Li^+).

The LTO with different particle sizes was prepared in such a way that nano-sized commercial-grade LTO having a primary particle size of ~30 nm was sintered from 700°C to 900°C. Atmosphere was controlled by flowing air to avoid the formation of undesirable oxygen defect. Notable growth of primary particles was observed after thermal treatment as shown in Fig. 2. From the comparison of morphologies for treated LTO at different temperatures, the primary particle size was effectively enlarged along with increasing treatment temperatures. The shape of secondary particles (inset) remains intact after thermal treatment. The primary particle sizes of treated LTO were estimated by SEM with values of ~500 nm (700°C), 1 μm (800°C), and 2 μm (900°C), respectively.

For further investigation, the structures of LTO were carefully refined by powder XRD analysis in Fig. 3. According to fine refinements, all reflections are in good accordance with a cubic symmetry which belongs to the space group of $Fd\bar{3}m$. There is no visible evidence for the formation of an impurity phase after the treatments. We only observed that all peaks were sharpened compared to those of bare sample indicating the

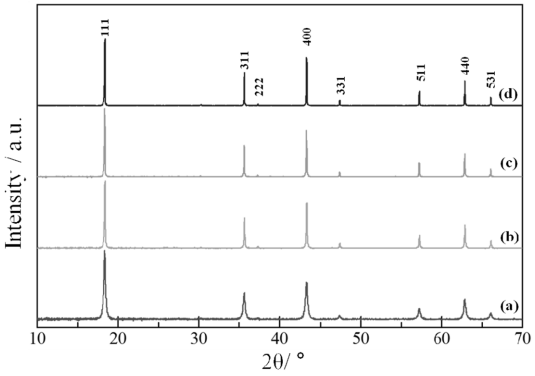

Fig. 3. XRD patterns of LTO heat-treated at different temperatures : (a) Bare, (b) 700°C, (c) 800°C, and (d) 900°C.

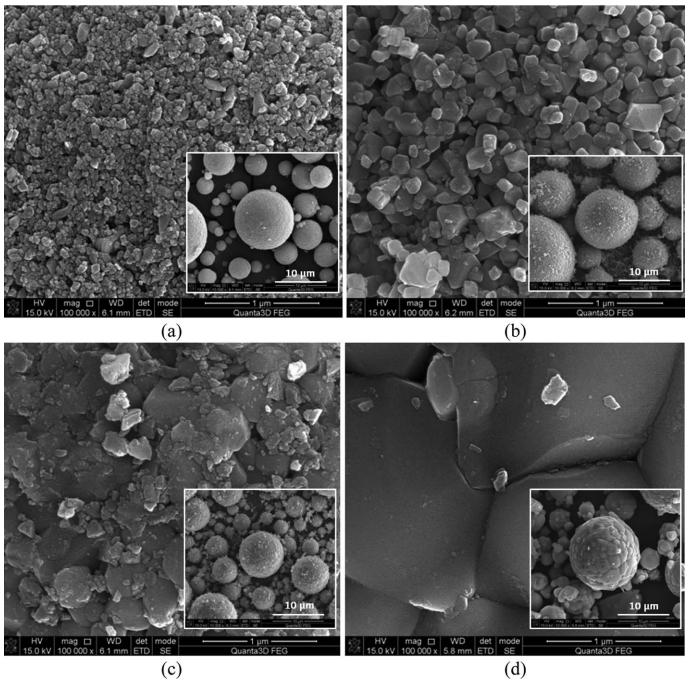

Fig. 2. SEM images of LTO heat-treated at different temperatures : (a) Bare, (b) 700°C, (c) 800°C, and (d) 900°C.

growth of crystallite size. The corresponding FWHM values for 400 reflection were calculated to be 0.094, 0.078, and 0.062 for the LTO treated at 700°C, 800°C, and 900°C, respectively. The reduction of FWHM value is a general characteristic induced by increasing crystallinity of a material when its grains are grown. It should be noted that the increase in particle size of LTO was originated from the grain growth without any compositional change.

The voltage profiles of treated LTO are presented in Fig. 4. Their electrochemical properties were carefully evaluated at the same conditions. All samples show similar charge profiles having a plateau around 1.59 V attributed to the Li^+ extraction from the host structure, $Li_{4+x}Ti_5O_{12}$ ($0 \le x \le 3$), due to the biphasic reaction between $Li_4Ti_5O_{12}$ and $Li_7Ti_5O_{12}$ based on the Gibbs phase rule.[3] However, major difference was observed in their discharge profiles where an additional 0.7 V plateau appeared during Li^+ insertion in the samples treated at 800°C and 900°C. The 0.7 V plateau was gradually elongated with increasing the particle size of LTO while the 1.56 V plateau was getting shorter during discharge. Interestingly, this behavior does not appear in the other samples (bare and 700°C). The overall delivered capacities are the same no matter what the sample kinds. We suspected that the plateau separation might be caused by particle size difference. It is expected that the plateau would be split if the particle size was decreased less than a critical scale determined by thermodynamic and kinetic factors in this system. Our findings give us more indication on the relationship between the particle size and electrochemical behavior of LTO.

A following point should be clarified whether it is mainly caused by the formation of intermediate phase or the diffusivity of Li^+ with a kinetic point of view to understand the reason for plateau separation during discharge. From this perspective, two approaches were employed to address a diagnosis for the origin of plateau separation occurred during discharge below 1.0 V. To implement our approaches, we selected two LTO with different particle sizes of 30 nm and 1 μm. Their structural variations and kinetic behaviors during discharge were carefully examined by *in-situ* XRD and OCV measurements. Fig. 5 shows *in-situ* XRD patterns

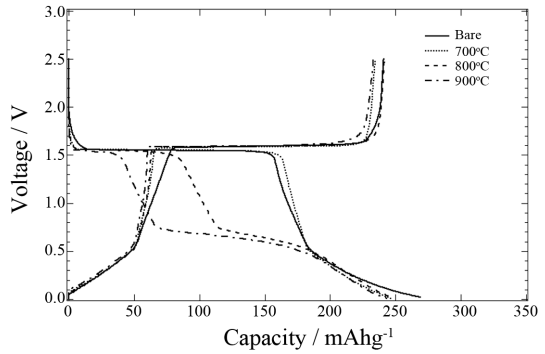

Fig. 4. Charge-discharge curves of LTO heat-treated at different temperatures.

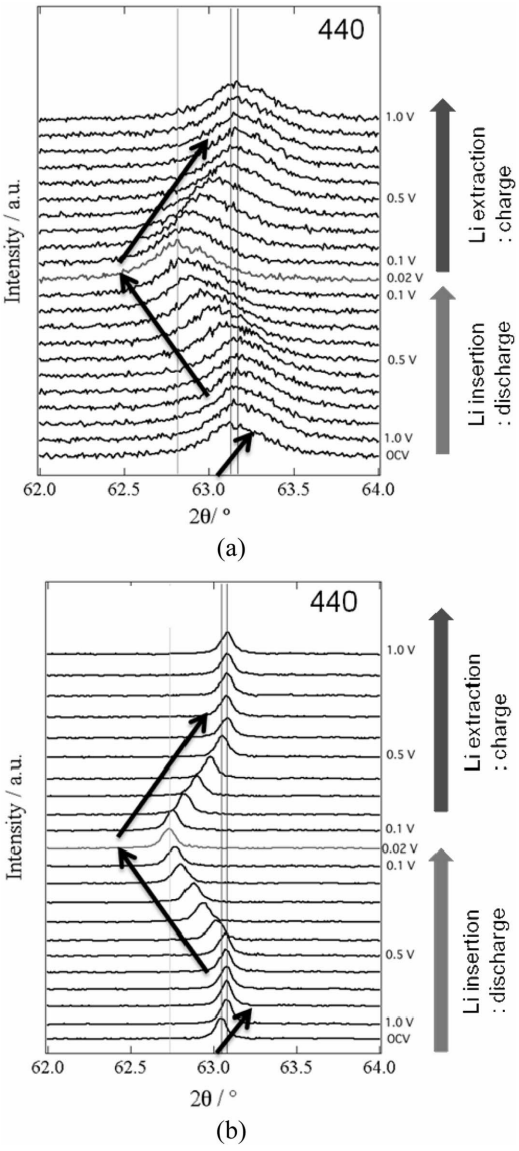

Fig. 5. In-situ XRD patterns of LTO with different primary particle size : (a) 30 nm and (b) 1 μm.

of 30 nm LTO and 1 μm LTO in the voltage of 0.02 V to 1.0 V during charge and discharge. As regard to 440 reflection, it is gradually shifted to the low angle during discharge from 1.0 V to 0.02 V. Then it is reversibly returned back to its original position when it charged up to 1.0 V. This peak shifting could be explained by two-step Li^+ insertion into the LTO system as follows; i) lattice shrinkage was accompanied with Li^+ insertion until 1.0 V, which is mainly attributed to the change of Li^+ position from 8a to 16c sites in the lattice and ii) 0.5% lattice expansion, due to the additional Li^+ occupancy in local 8a sites to form $Li_{8.5}Ti_5O_{12}$, is introduced when it was discharged to 0.02 V.[13-15] Regardless of their particle sizes, both LTOs show a similar behavior and the formation of an intermediate phase was not detected in the *in-situ* XRD patterns. This result indicates that the plateau separation is not induced by the formation of an intermediate phase or structural deformation during discharge.

To make sure the effects of kinetic limitations of Li^+ on the plateau separation, the rate characteristics of 30 nm LTO and 1 μm LTO was evaluated as illustrated in Fig. 6. The 30 nm LTO shows only one plateau corresponding to the biphasic reaction even at high C-rate discharge through the whole range of discharge while the discharge plateau of 1 μm LTO was separated. In case of 1 μm LTO, the additional plateau at 0.7 V was elongated as applied current is increased from 0.2C to 2C which indicates that the plateau separation is highly depending on Li^+ diffusivity of LTO. This important observation motivated to check their electrochemical stability during discharge. OCV profiles of 30 nm LTO and 1 μm LTO were compared when Li^+ is inserted into the host structure in Fig. 7. Unlike 30 nm LTO sample, huge voltage relaxations have been observed in the 1 μm LTO indicating a limited Li^+ diffusion. Those relaxations were occurred in a specific depth of discharge (DOD) region of X = 1.2 to X = 3.0 in $Li_{4+x}Ti_5O_{12}$, corresponding to the biphasic reaction rather than additional Li^+ insertion. It is interesting to note that the plateau separation could be mainly determined by Li^+ diffusivity during the biphasic reaction between spinel and rock-salt structures. According to the Fick's second law, the Li^+ diffusion

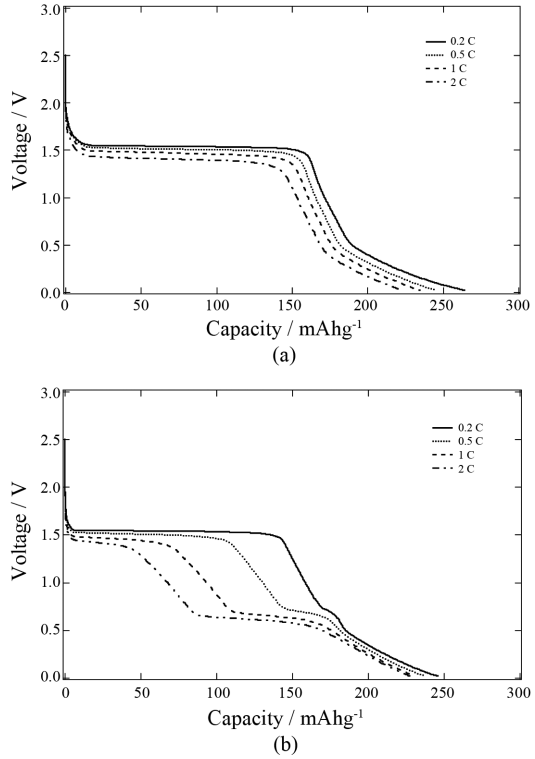

Fig. 6. Rate capability of LTO with different primary particle size : (a) 30 nm and (b) 1 μm.

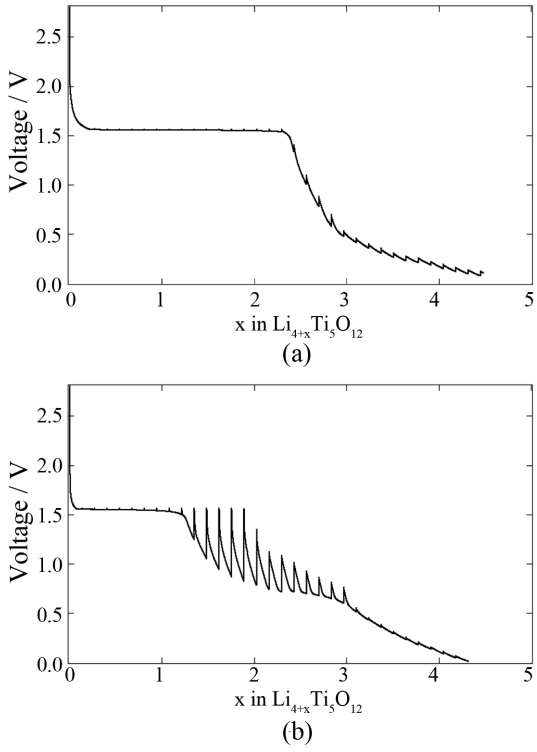

Fig. 7. Open circuit voltage of LTO with different primary particle size : (a) 30 nm and (b) 1 μm.

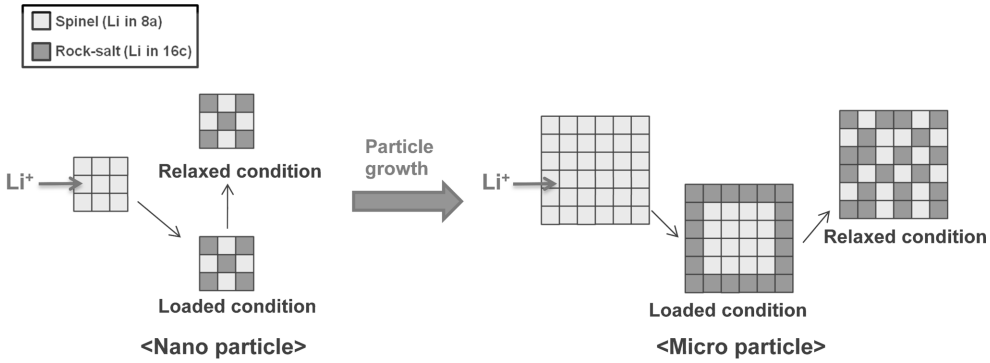

Fig. 8. Schematic for the different Li diffusion kinetics of nano and micro LTO particles.

length determined by particle size is responsible for Li^+ diffusivity because the smaller particle provides the shorter Li^+ diffusion length compared to that of larger particle.[12)]

Based on their structural and electrochemical verifications, we suggest a model of electrochemical plateau separation in Fig. 8. A schematic diagram describes a possible reaction mechanism in the DOD region of $X = 1.2$ to $X = 3.0$ in $Li_{4+x}Ti_5O_{12}$. The Li^+ could be easily diffused at the surface and bulk in its nanoscale form. However, more stress would be introduced if the particle were large leading to the increase of resistance for Li^+ diffusion.

As a result, the concentration of Li^+ would be increased at the surface because of the diffusion limitation of Li^+ moving into the bulk structure. For this reason, the plateau could be separated to 1.5 V and 0.7 V during discharge. Both plateaus have same origin and reaction mechanism but different voltages resulted from the limitation of Li+ diffusion caused by diffusion length. Authors can come to conclude that the plateau separation is mainly originated from the Li^+ kinetics related to its particle size rather than formation of an intermediate phase in the LTO system.

4. Conclusions

The mean free path of Li^+ diffusion is considered as an important kinetic factor affecting the electrochemical behavior of lithium titanate, $Li_4Ti_5O_{12}$ (LTO). Herein, we describe a possible reaction model to elucidate the abnormal plateau separation below 1.0 V (vs. Li/Li^+) based on the systematic verifications. As the length of diffusion path of Li^+ is increased, the plateau is elongated which means the resistivity for Li^+ insertion is increasing at the surface and bulk of LTO. Therefore, it is evident that the formation of additional 0.7 V plateau is strongly related to the particle size of LTO and the plateau does not seem to correlate with the formation of a new intermediate phase during discharge.

Acknowledgements

This work was performed in the R&D program “Development of Anode Materials for kWh-grade Energy Storage” by financial support from Ministry of Knowledge Economy and greatly appreciated to analyze the SEM images from “Center for Innovation in Advanced Batteries” by same financial support.

References

1. T. Ohzuku, A. Ueda and N. Yamamoto, *J. Electrochem. Soc.*, **142**, 1431 (1995).
2. K. Ariyoshi, R. Yamanoto and T. Ohzuku, *Electrochim. Acta*, **51**, 1125 (2005).
3. S. Scharner, W. Weppner and P. Schmid-Beurmann, *J. Electrochem. Soc.*, **146**, 857 (1999).
4. S. Panero, P. Reale, F. Ronci, B. Scrosati, P. Perfetti and V. R. Albertini, *PCCP*, **3**, 845 (2001).
5. F. Ronci, P. Reale, B. Scrosati, S. Panero, V. R. Albertini, P. Perfetti, M. di Michiel and J. M. Merino, *J. Phys. Chem. B*, **106**, 3082 (2002).
6. W. Lu, I. Belharouak, J. Liu and K. Amine, *J. Electrochem. Soc.*, **154**, A114 (2007).
7. A. D. Robertson, H. Tukamoto and J. T. S. Irvine, *J. Electrochem. Soc.*, **146**, 3958 (1999).
8. S. Huang, Z. Wen, X. Zhu and Z. Lin, *J. Power Sources*, **165**, 408 (2007).
9. K. C. Hsiao, S. C. Liao and J. M. Chen, *Electrochim. Acta*, **53**, 7242 (2008).
10. X. L. Yao, S. Xie, H. Q. Nian and C. H. Chen, *J. Alloys*

Comp, **465**, 375 (2008).
11. W. J. H. Borghols, M. Wagemaker, U. Lafont, E. M. Kelder and F. M. Mulder, *J. Am. Chem. Soc*., **131,** 17786 (2009).
12. A. Van der Ven and M. Wagemaker, *Electrochem. Commun.* , **11**, 881 (2009).
13. C. Y. Ouyang, Z. Y. Zhong and M. S. Lei, *Electrochem Commun*., **9**, 1107 (2007).
14. L. Aldon, P. Kubiak, M. Womes, J. C. Jumas, J. O. Fourcade, J. L. Tirado, J. I. Corredor and C. P. Vicente, *Chem. Mater*. **16**, 5721 (2004).
15. Z. Y. Zhong, C. Y. Ouyang, S. Q. Shi and M. S. Lei, *Chem Phys Chem*., **9**, 2104 (2008).